Int J Clin Exp Pathol 2015;8(7):7685-7693
www.ijcep.com /ISSN:1936-2625/IJCEP0010023

Original Article

Ulinastatin mediates protection against vascular hyperpermeability following hemorrhagic shock

Bo Lin[1*], Youtan Liu[2*], Tao Li[3], Kai Zeng[1], Shumin Cai[4], Zhenhua Zeng[4], Caizhu Lin[1], Zhongqing Chen[4], Youguang Gao[1]

[1]*Department of Anesthesiology, The First Affiliated Hospital of Fujian Medical University, Fuzhou 350005, China;* [2]*Department of Anesthesiology, Shenzhen Hospital, Soutern Medical University, Shenzhen 518110, China;* [3]*Department of Critical Care Medicine, The First People's Hospital of Chenzhou, Institute of Translation Medicine, Chenzhou 423000, China;* [4]*Department of Critical Care Medicine, Nanfang Hospital, Southern Medical University, Guangzhou510515, China.* [*]*Equal contributors.*

Received May 8, 2015; Accepted June 25, 2015; Epub July 1, 2015; Published July 15, 2015

Abstract: Object: Recent studies have suggested that intrinsic apoptotic signaling cascade is involved in endothelial barrier dysfunction following hemorrhagic shock (HS), which results in vascular hyperpermeability. Our previous study demonstrated that ulinastatin (UTI) inhibits oxidant-induced endothelial hyperpermeability and apoptotic signaling. In present study, we hypothesized that UTI would improve HS-induced vascular hyperpermeability by regulating the intrinsic apoptotic signaling cascade. Methods: Hemorrhagic shock was induced in rats by withdrawing blood to reduce the mean arterial pressure to 40-45 mmHg for 60 min, followed by reperfusion. Mesenteric postcapillary venules were examined for changes in hyperpermeability by intravital microscopy. In vitro, Rat lung microvascular endothelial cells (RLMVECs) were exposed in hemorrhagic shock serum for 120 min, followed by transendothelial electrical resistance (TER) estimation. Mitochondrial release of cytochrome c and caspase-3 activation was estimated in vivo. In vitro, ratio of cell apoptosis was evaluated by Annexin-V/PI double stain assay; mitochondrial membrane potential ($\Delta\Psi_m$) was determined with JC-1; intracellular ATP content was assayed by a commercial kit; reactive oxygen species (ROS) was measured by DCFH-DA; adherens junction protein β-catenin was detected by immunofluorescense staining. Results: In vivo, UTI attenuated HS-induced vascular hyperpermeability versus the HS group ($P < 0.05$); In vitro, UTI attenuated shock serum induced RLMEC monolayer hyperpermeability ($P < 0.05$). In vivo, UTI inhibited HS-induced cytochrome *c* release and caspase-3 activation ($P < 0.05$). In vitro, shock serum induced cell apoptosis, low ATP level, $\Delta\Psi_m$ depolarization, ROS increase were improved by UTI pre-treatment ($P < 0.05$). UTI improved shock serum induced disruption of endothelial cell adherens junction. Conclusions: UTI inhibits vascular hyperpermeability following HS. UTI regulates oxidative stress and intrinsic apoptotic signaling following HS.

Keywords: Hemorrhagic shock, hyperpermeability, ulinastatin, apoptosis, mitochondria

Introduction

Vascular hyperpermeability occurring after certain conditions, such as hemorrhagic shock (HS), is caused by disruption of the endothelial cell barrier [1, 2]. Recent studies have suggested that intrinsic apoptotic signaling cascade is involved in endothelial dysfunction, which may result in hyperpermeability following HS [3-5].

The intrinsic apoptotic pathway is mediated through the mitochondrial release of cytochrome c, second mitochondrial derived activator of caspases (smac), and apoptosis-inducing factor (AIF) [6, 7]. Translocations of smac and cytochrome *c* from mitochondria to the cytosol through mitochondrial transition pores are important routes of caspase activation [8]. Caspase-3 has been shown to cleave β-catenin, thereby disrupting the vascular endothelial (VE)-cadherin-β-catenin complex, which serves as a key role of cell-cell adhesion in endothelial cells [9].

Ulinastatin (UTI), mainly used in the treatment of sepsis, shock, pancreatitis, and ischemia-reperfusion injury, has been reported the protective effects against apoptosis via mitochon-

dria protection [10-14]. In addition, our previous study demonstrated that UTI inhibits oxidant-induced endothelial hyperpermeability and apoptotic signaling in vitro [4]. In present study, we hypothesized that UTI would improve HS-induced vascular hyperpermeability by regulating the intrinsic apoptotic signaling cascade.

Materials and methods

Experimental animals

The procedures used in this study and the handling of study animals adhered to the National Institutes of Health guidelines on the use of experimental animals. The experimental protocol was approved by the Committee on Research Animal Use of Fujian Medical University. Male Sprague-Dawley rats weighing 180-220 g were purchased from the Experimental Animal Center at Fujian Medical University and allowed to acclimatize for a week before being used. Animals had ad libitum access to chow and water.

Animal surgery and intravital microscopy

Rats were intramuscularly anesthetized with an injection of sodium pentobarbital (30 mg/kg). Mean arterial blood pressure (MAP) was continuously measured using a PE-50 cannula in femoral artery. The second cannula in femoral vein was used to administer drugs and blood, while the third cannula placed in another femoral artery was used for blood withdrawal. The rats were placed in a lateral decubitus position on a temperature-controlled Plexiglas platform mounted to an intravital upright microscope (ECLIPSEFN1, Nikon, Japan). The mesentery was maintained at 37°C. The mesentery was superfused with normal saline at 2 ml/min and covered with plastic wrap to reduce evaporation. Venules with diameters of 20-35 μm were selected for study (100 × magnification).

Vascular permeability measurement

The rats were allowed to recover from surgical manipulation for 30 min before the start of all experiments. During this period, the animals were dosed with FITC-albumin (50 mg/kg) and baseline-integrated optical intensities were obtained intra- and extra-vascularly (2 sites, same computed areas; mean values were used). The rats were divided into: control (sham) group, HS group and UTI group (pretreated with 50,000 u/kg UTI). Each experimental group consisted of six rats. The experimental groups of animals then underwent 60 min of hemorrhagic shock. To produce hemorrhagic shock, MAP was decreased to 40 mmHg by withdrawing blood from the right carotid artery into a syringe containing 100 U of heparin. After the shock period, the shed blood plus two times the volume of normal saline was reinfused to maintain a MAP ≥ 90 mmHg. Parameters were recorded after shock at 10-min intervals for 60 min.

The extravasation of FITC-albumin was measured by determining the changes in integrated optical intensity by image analysis: $\Delta I = 1-(Ii-Io)/Ii$, where ΔI is the change in light intensity, Ii is the light intensity inside the vessel, and Io is the light intensity outside the vessel. The labeled albumin (FITC) represented relative change in permeability. Areas in the small bowel mesentery, postcapillary venules, and the adjacent extravascular space were selected for study. The images were standardized to images taken at the beginning of each experiment within the same animal and at selected timed intervals between different animals.

Monolayer permeability

Rat lung microvascular endothelial cells (RLMVECs, ScienCell, USA) were maintained in DMEM/F12 containing 10% fetal bovine serum at 37°C in a humidified atmosphere with 5% CO_2-95% air. In all experiments, RLMVECs were grown to 90% confluence and starved of serum for 12 hours before being stimulated with H_2O_2. The monolayers were respectively pretreated with 50 000 u/L of UTI for 60 min, followed by stimulation of serum. DMEM/F12 was used as vehicle control. Finally, endothelial permeability was measured following 120 min stimulation.

Arterial blood was withdrew and stewing for 30 min from rats after 60 min-HS (or sham), subsequently centrifuged at 3000 r/min for 10 min to obtain serum.

Transendothelial electrical resistance (TER)

Transendothelial electrical resistance (TER) of HUVECs monolayer was determined using STX2 electrode and EVOM2 meter according to the

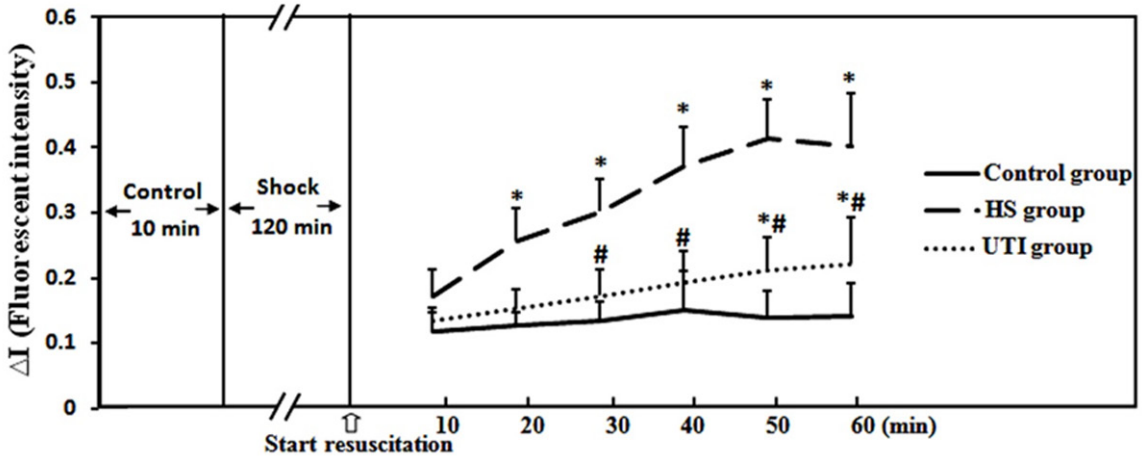

Figure 1. UTI decreases HS-induced vascular hyperpermeability in rat mesentery postcapillary venules. Vascular permeability is expressed as change in fluorescent intensity inside the vessel compared with the intensity outside the vessel. Data are presented as mean ± SD (n = 6 in each group). *P < 0.05 versus the sham group; #P < 0.05 versus the shock+ NS group.

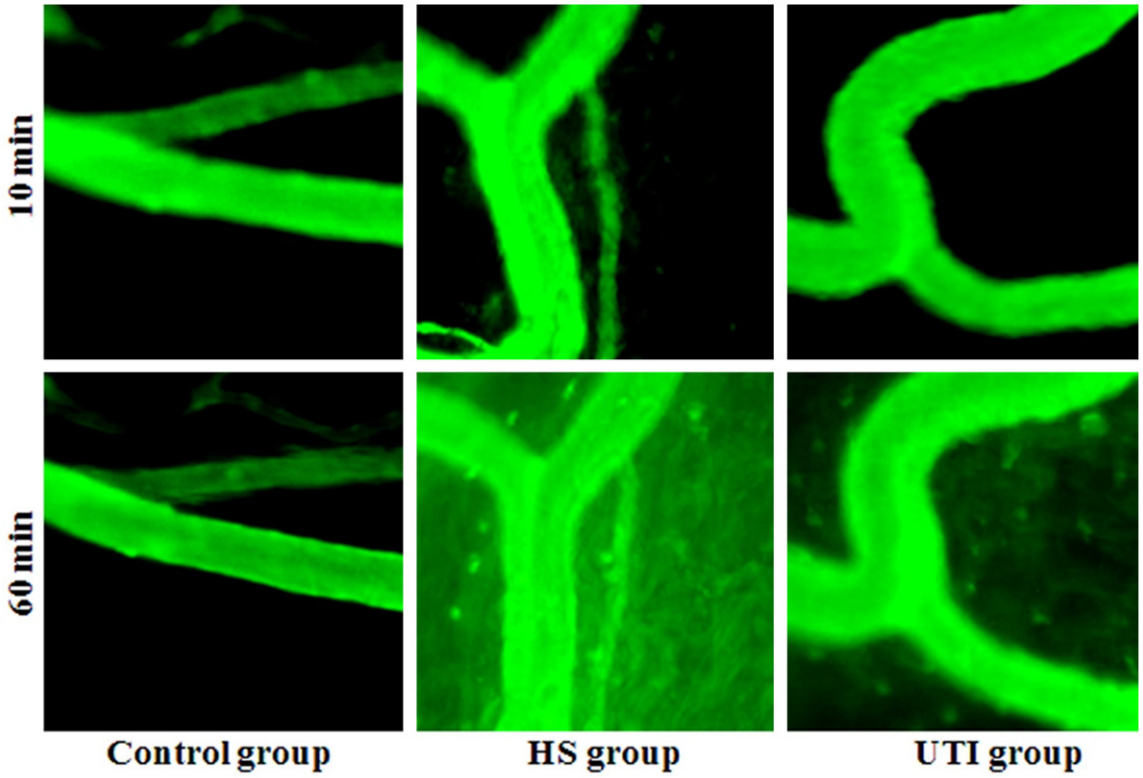

Figure 2. UTI attenuates HS-induced FITC-albumin extravasation in rat mesenteric postcapillary venules. The images of mesenteric postcapillary venules are shown. The FITC-albumin extravasation into the extravascular space is observed after HS, whereas UTI treatment prevented the extravasation.

instruction manual of manufacture (World Precision Instruments, Sarasota, FL, USA) [15]. HUVECs were seeded with number of 1 × 10^5/cm^2 on fibronectin-coated, 6.5 mm Transwell filters (0.4 mm pore size) and were used until full confluence. Resistance values of multiple Transwell inserts of an experimental group were measured sequentially and the mean was

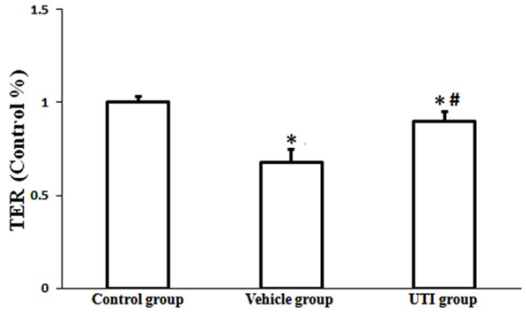

Figure 3. UTI attenuates HS-induced endothelial hyperpermeability. RLMVECs were stimulated by shock serum. Permeability was examined by detecting the TER of RLMVECs monolayer. Data are presented as mean ± SD (n = 6 in each group). *P < 0.05, versus the control group; #P < 0.05, versus the vehicle group.

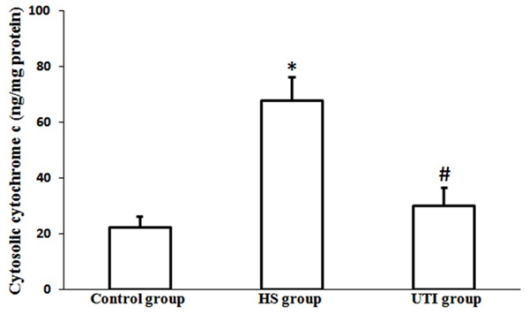

Figure 4. UTI inhibits HS-induced cytochrome *c* release in vivo. Cytosolic cytochrome *c* levels were estimated using a cytochrome *c* ELISA kit. Data are presented as mean ± SD (n = 6 in each group). *P < 0.05, versus the control group; #P < 0.05, versus the vehicle group.

expressed in the common unit (Ω cm^2) after subtraction of the value of a blank cell-free filter.

Measurement of cytosolic cytochrome c in vivo

Cytosolic cytochrome *c* levels were estimated with a cytochrome *c* ELISA kit. The mesenteric microvasculature were dissected from rats after HS (or sham), weighed, and lysed in a cold preparation buffer (10 mM Tris-HCl, 0.3 M sucrose, 10 μM aprotinin, 10 μM pepstatin, 10 μM leupeptin, and 1 mM PMSF, pH 7.5). The tissue homogenates were centrifuged (10,000 *g* for 60 min at 4°C), and the supernatant (cytosol fraction) was collected and subjected to protein estimation (BCA method). Then, the samples were treated with a conjugate reagent, transferred to a cytochrome *c* antibody-coated microwell plate, and incubated at room temperature for 60 min. The wells were washed and treated with a substrate and incubated for 30 min, followed by addition of a stop solution. The optical density was read at 450 nm using an automatic microplate reader (SpectraMax M5; Molecular Devices, Sunnyvale, CA, USA). A serial dilution of cytochrome *c* calibrator was subjected to the assay along with the samples, the values were plotted, and the concentration of cytochrome *c* was calibrated from the standard curve.

Measurement of cleaved caspase-3 expression in vivo

The rat mesenteric microvasculature was dissected from rats after HS (or sham). The tissues were homogenated and analyzed for cleaved caspase-3 by western blotting. Protein concentrations were determined using the BCA method. An equal amount of protein was loaded onto 10% sodium dodecyl sulphate polyacrylamide gel for electrophoresis. After electrophoresis, proteins were electroblotted onto polyvinylidene fluoride membranes and blotted with primary antibodies against cleaved caspase-3 (Abcam, UK). Membranes were then incubated with the horseradish peroxidase-tagged secondary antibody (Tianjin Sungene Biotech Co., Ltd. Tianjin, China), and protein expression was detected using an enhanced chemiluminescence reagent.

Measurement of cell apoptosis in vitro

Cell apoptosis were detected by an Annexin V-FITC apoptosis detection kit (BD Biosciences, USA). After induction with serum, cells were washed twice with PBS and suspended in 1× binding buffer at a concentration of approx 1 × 10^5 cells/ml. 5 μl of FITC-Annexin V and 10 μl of propidium iodide (PI, 50 μg/ml, Sigma) was added to cell suspension. After incubation at room temperature for 20 minutes at dark, the fluorescence of the cells was determined immediately with a flow cytometer (Becton Dickinson FACScan, San Jose, CA).

Measurement of mitochondrial membrane potential in vitro

The mitochondrial membrane potential ($\Delta\Psi_m$) was determined by flow cytometry, using the potential-sensitive fluorescent dye JC-1. The color of this dual-emission probe changed from red-orange to green as the mitochondrial mem-

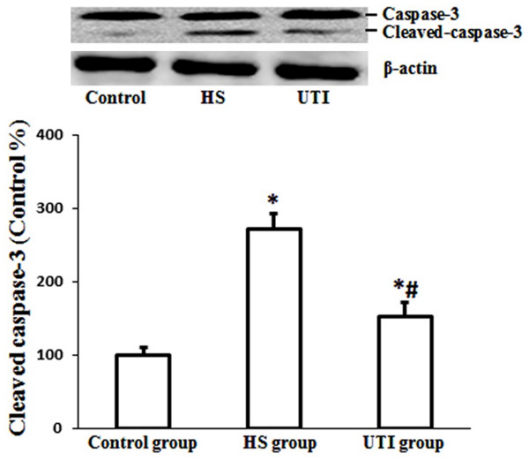

Figure 5. UTI decreases HS-induced caspase-3 activation. The cleaved caspase-3 was measured by Western blot. Above, Representative Western blots for cleaved caspase-3. Under, Protein quantification by densitometry. Data are presented as mean ± SD (n = 6 in each group). *P < 0.05, versus the control group; #P < 0.05, versus the vehicle group.

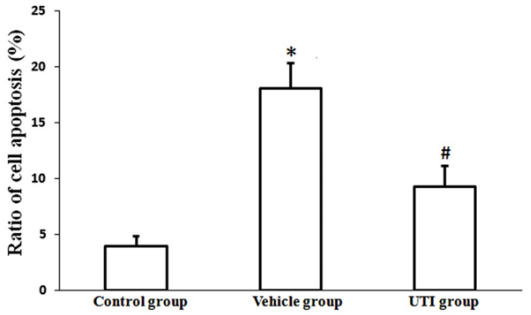

Figure 6. UTI inhibits HS-induced cell apoptosis in vitro. Ratio of cell apoptosis was evaluated by Annexin-V/PI double stain assay and analyzed by flow cytometry. Data are presented as mean ± SD (n = 6 in each group). *P < 0.05, versus the control group; #P < 0.05, versus the vehicle group.

brane turned depolarized. The JC-1 (5 μmol/L) was loaded onto RLMVECs for 15 min at 37°C. The stained cells were washed with PBS, and analyzed by flow cytometry (Becton Dickinson FACScan). A minimum of 10,000 cells per sample was analyzed. JC-1 monomers emit at 527 nm and "J-aggregates" emit at 590 nm. The percentage of cells with abnormally low $\Delta\Psi_m$ (green fluorescence) was determined.

Measurement of cellular ATP in vitro

Intracellular ATP was determined by a luciferase-based assay (CellTiter-Glo, Madison, WI), according to the manufacturer's recommendation. After adding 100 μL of the CellTiter-Glo reagent to 100 μL of cells suspension containing 10,000 cells in each well of a standard opaque-walled 96-well plate, the plates were allowed to incubate at room temperature for 10 min and the luminescence was recorded in an automatic microplate reader (SpectraMax M5).

Measurement of ROS levels in vitro

Intracellular ROS levels were assessed using DCFH-DA probe (Sigma, USA). Cells were treated with DCFH-DA (10 μM), following HS serum, for 20 mins at 37°C. After incubation, the cells were washed and analyzed using an automatic microplate reader (Spectra Max, M5). The relative intensity of DCF fluorescence was determined at a wavelength of 535 nm as compared to sham group cells.

Statistical analysis

All variables are presented as means ± s.d. Differences between groups were determined using one-way ANOVA with the LSD multiple-comparison test and Student's *t*-test when appropriate. Values were considered significant when P < 0.05.

Results

UTI attenuates HS-induced vascular hyperpermeability

Hemorrhagic shock-induced vascular leak was evidenced by a significant increase in extravasation of FITC-albumin into the extravascular space versus the control group (P G 0.05; n = 5; **Figures 1** and **2**). UTI significantly attenuated HS-induced vascular leak compared with the HS group (P G 0.05; n = 5; **Figures 1** and **2**).

Figure 1 is a graphic representation of the changes in vascular leak. The change in vascular leak is expressed as change in fluorescent intensity inside the vessel versus fluorescent intensity outside the vessel. HS induced a significant increase in FITC-albumin extravasation (P G 0.05; n = 5). UTI pretreatment significantly decreased vascular leak (P G 0.05; n = 5).

Figure 2 is a series image of a rat mesenteric postcapillary venule. In control, minimal extravasation of FITC-albumin into the extravascular

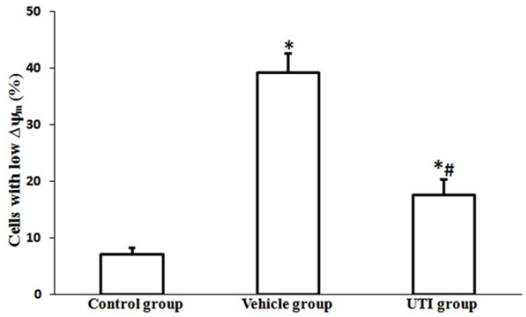

Figure 7. UTI inhibits HS-induced loss of mitochondrial membrane potential ($\Delta\Psi_m$) in vitro. The $\Delta\psi_m$ was measured using the fluorescent probe JC-1 and analyzed by flow cytometry. Data are presented as mean ± SD (n = 6 in each group). *P < 0.05, versus the control group; #P < 0.05, versus the vehicle group.

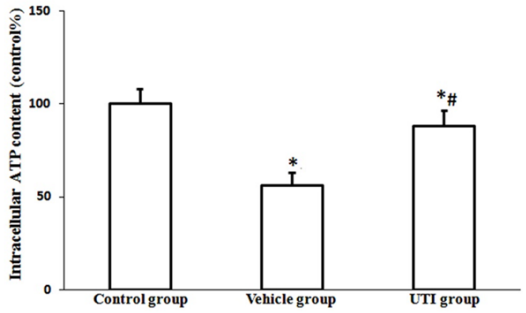

Figure 8. UTI improves HS-induced mitochondrial dysfunction in vitro. Cells' ATP level was determined by a luciferase-based assay. Data are presented as mean ± SD (n = 6 in each group). *P < 0.05, versus the control group; #P < 0.05, versus the vehicle group.

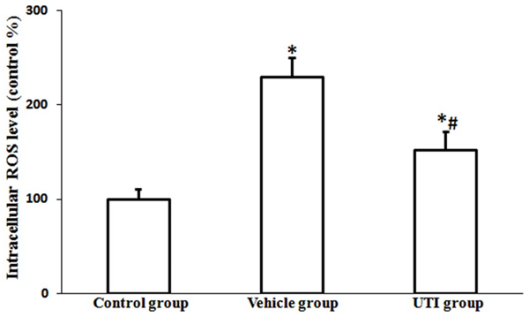

Figure 9. UTI reduces HS-induced ROS generation in vitro. Intracellular ROS levels were assessed using DCFH-DA probe. Data are presented as mean ± SD (n = 6 in each group). *P < 0.05, versus the control group; #P < 0.05, versus the vehicle group.

space was observed. After HS, a marked increase of FITC-albumin extravasation was detected in HS group compared with control group, which was reduced by UTI treatment.

UTI attenuates HS-induced endothelial hyperpermeability

As shown in **Figure 3**, HS-induced monolayer hyperpermeability was evidenced by an obvious decrease in the TER of the cell monolayer in HS group compared to that of the cell monolayer in the control group; the hyperpermeability was significantly attenuated by UTI pretreatment.

UTI prevents HS-induced cytochrome c release in vivo

The release of cytochrome c from the mitochondria into the cytosol has been reported to be the key event in the intrinsic apoptosis cascade induced by various stimuli. The cytosolic cytochrome *c* level in mesenteric vascular tissue was elevated after HS compared with the control group (P G 0.05; n = 5). The HS animals pretreated with UTI showed a significantly lower level of cytosolic cytochrome *c* compared with the HS group (P G 0.05; n = 5; **Figure 4**).

UTI decreases HS-induced caspase-3 activation in vivo

Caspase-3 activation occurs after cytochrome *c* release from mitochondria. Caspase-3 activation leads to the proteolytic cleavage of a variety of cellular substrates including endothelial cell adherens junction proteins. So, cleaved caspase-3 was determined from the rat mesenteric vasculature. The HS group showed a significant up-regulation of cleaved caspase-3 compared with the control group (P G 0.05; n = 5; **Figure 5**). Then, UTI prevented the HS-induced up-regulation of cleaved caspase-3 compared with HS group (P G 0.05; n = 5; **Figure 5**).

UTI reduces HS-induced endothelial cell apoptosis in vitro

Rates of cell apoptosis were markedly increased in the vehicle group compared with the control group (**Figure 6**; P < 0.05). In contrast, the alterations were improved by the UTI treatment group (**Figure 6**; P < 0.05).

UTI inhibits HS-induced loss of mitochondrial transmembrane potential ($\Delta\Psi_m$) in vitro

We determined the $\Delta\Psi_m$ using JC-1. Cells were incubated with JC-1 and the mitochondrial

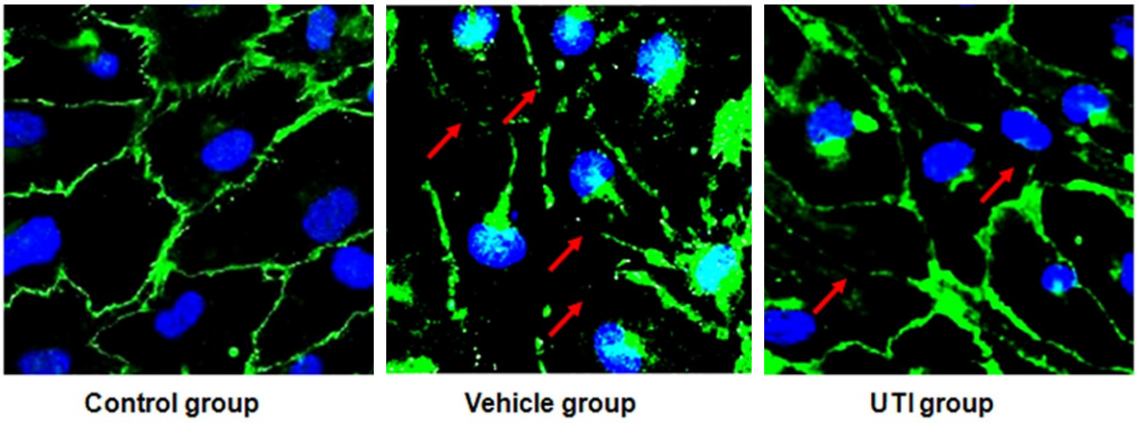

Figure 10. UTI inhibits HS-induced disruption of endothelial cell adherens junction in vitro. Adherens junction protein β-catenin was detected by immunofluorescense staining. Red arrow: disruption of the junctions evidenced by irregular and scattered β-catenin fluorescence.

membrane potential was evaluated by flow cytometry. Cell with low $\Delta\Psi_m$ increased in the HS group compared with control group (**Figure 7**; $P < 0.05$). The cell pretreated with UTI showed a significantly lower level of cell with low $\Delta\Psi_m$ compared with vehicle group (P G 0.05; n = 5; **Figure 7**).

UTI improves HS-induced mitochondrial dysfunction in vitro

In the vehicle group, the intracellular ATP level was remarkable decreased compared with control group (**Figure 8**; $P < 0.05$ *vs.* control group), indicating mitochondrial dysfunction following serum stimulation. Pretreatment with the UTI improved HS-induced the ATP level decrease (**Figure 8**; $P < 0.05$ *vs.* vehicle group).

UTI reduces HS-induced ROS increase in vitro

Intracellular ROS levels were assessed using DCFH-DA probe. HS resulted in a significant increase in ROS formation compared with the control group (P G 0.05; **Figure 9**). UTI pretreatment resulted in significant attenuation of ROS formation compared with the vehicle group (P G 0.05; **Figure 9**).

UTI inhibits HS-induced disruption of adherens junctions

Control cells showed strong and continuous β-catenin immunofluorescence at the cell-cell junctions, indicating an intact cell barrier. In contrast, treatment with HS serum disrupted the cell junctions among cells as evidenced by the irregular and scattered β-catenin fluorescence observed. However, the alterations induced by HS serum were improved by UTI pretreatment (**Figure 10**).

Discussion

It has been shown that mitochondrial ROS formation, activation of intrinsic apoptotic signaling, and vascular hyperpermeability occur following HS [1, 5, 16]. This study supports our hypothesis that UTI effectively inhibits HS-induced vascular hyperpermeability, cellular ROS formation, mitochondrial membrane depolarization, mitochondrial release of cytochrome c, activation of caspase 3, and disruption of adherens junctions.

Hemorrhagic shock is known to induce vascular hyperpermeability. In this study we applied intravital microscopy along with digital imaging to characterize the changes in fluorescein labeled protein transport in the shock rat mesenteric venula. We demonstrated UTI significantly attenuated vascular hyperpermeability following hemorrhagic shock. In parallel studies conducted in vitro, UTI inhibited shock serum-induced monolayer hyperpermeability.

Recent studies demonstrated a decrease in mitochondrial transmembrane potential, release of cytochrome c from mitochondria, and activation of caspase 3 in association with vascular hyperpermeability after HS [1, 4, 17]. These results suggested that an effective

approach to control vascular hyperpermeability after HS may be to protect the mitochondrial transition pores and prevent cytochrome c release and subsequent caspase 3 activation. In our past study, we demonstrated that UTI Inhibits oxidant-induced endothelial hyperpermeability and apoptotic signaling in vitro [4]. Thus, the main purpose of the present study was to test whether UTI can inhibit the intrinsic apoptotic signaling in HS. Our results suggest that UTI protected HS-induce mitochondrial dysfunction, which is evident from the prevention of mitochondrial transmembrane potential depolarization and cellular ATP level decrease. Various mitochondrial functions require an intact mitochondrial transmembrane potential [18, 19]. Mitochondria damage and mitochondrial transmembrane depolarization lead to the mitochondrial release of cytochrome *c* [20, 21]. After the release to the cytosol, cytochrome *c* mediates the allosteric activation of apoptotic protease activating factor 1, which is required for the proteolytic maturation of caspase 9 and caspase 3 [22-24]. So, the caspase 3 activation observed in our study may be explained as a result of an increased mitochondrial release of cytochrome c. The present study shows that UTI can prevent cytochrome c release and caspase-3 activation after HS. The observation that UTI prevented cell apoptosis further shows the protective effects of UTI against intrinsic apoptosis following HS.

Oxidative stress is one of the most important mediators of apoptotic signaling and subsequent cell death, and has been implicated in HS [25, 26]. Our results show that UTI inhibited HS-induced mitochondrial ROS formation. It is quite possible that in HS-induced vascular permeability, mitochondrial oxidative stress played an important role in the release of cytochrome c to the cytoplasm. UTI, by its antioxidant activity, might have prevented this effect.

Caspase-3 activation has been shown to result in the cleavage of a variety of cell adherens proteins including β-catenin [9, 17]. In endothelial cells, β-catenin functions as a regulator of cadherin-mediated cell-cell adhesion. From immunofluorescence staining, we find that shock serum cause irregular and scattered β-catenin fluorescence, which was improved by UTI treatment.

In conclusion, our findings show that UTI inhibits its HS-induced vascular leak. This protective effect of UTI on the vascular permeability is at least partially mediated through the inhibition of the mitochondrial mediated intrinsic apoptotic signaling pathway.

Disclosure of conflict of interest

None.

Address correspondence to: Dr. Youguang Gao, Department of Anesthesiology, The First Affiliated Hospital of Fujian Medical University, 20 Chazhong Road, Fuzhou 350005, China. E-mail: gaoyouguang259@163.com; Dr. Zhongqing Chen, Department of Critical Care Medicine, Nanfang Hospital, Southern Medical University, 1838 Guangzhou Avenue North, Guangzhou 510515, China. E-mail: czq_icu@163.com

References

[1] Sawant DA, Tharakan B, Hunter FA, Childs EW. The role of intrinsic apoptotic signaling in hemorrhagic shock-induced microvascular endothelial cell barrier dysfunction. J Cardiovasc Transl Res 2014; 7: 711-718.

[2] Peng Z, Pati S, Potter D, Brown R, Holcomb JB, Grill R, Wataha K, Park PW, Xue H, Kozar RA. Fresh frozen plasma lessens pulmonary endothelial inflammation and hyperpermeability after hemorrhagic shock and is associated with loss of syndecan 1. Shock 2013; 40: 195-202.

[3] Childs EW, Tharakan B, Hunter FA, Smythe WR. 17β-estradiol mediated protection against vascular leak after hemorrhagic shock. Shock 2010; 34: 229-235.

[4] Li G, Li T, Li Y, Cai S, Zhang Z, Zeng Z, Wang X, Gao Y, Li Y, Chen Z. Ulinastatin inhibits oxidant-induced endothelial hyperpermeability and apoptotic signaling. Int J Clin Exp Pathol 2014; 7: 7342-7350.

[5] Tharakan B, Corprew R, Hunter FA, Whaley JG, Smythe WR, Childs EW. 17β-estradiol mediates protection against microvascular endothelial cell hyperpermeability. Am J Surg 2009; 197: 147-154.

[6] Kumar R, Han J, Lim HJ, Ren WX, Lim JY, Kim JH, Kim JS. Mitochondrial induced and self-monitored intrinsic apoptosis by antitumor theranostic prodrug: in vivo imaging and precise cancer treatment. J Am Chem Soc 2014; 136: 17836-17843.

[7] Li K, Li Y, Shelton JM, Richardson JA, Spencer E, Chen ZJ, Wang X, Williams RS. Cytochrome c deficiency causes embryonic lethality and at-

tenuates stress-induced apoptosis. Cell 2000; 101: 389-399.
[8] Kamba AS, Ismail M, Ibrahim TA, Zakaria ZA, Gusau LH. In vitro ultrastructural changes of MCF-7 for metastasise bone cancer and induction of apoptosis via mitochondrial cytochrome C released by CaCO3/Dox nanocrystals. Biomed Res Int 2014; 2014: 391869.
[9] Childs EW, Tharakan B, Hunter FA, Tinsley JH, Cao X. Apoptotic signaling induces hyperpermeability following hemorrhagic shock. Am J Physiol Heart Circ Physiol 2007; 292: H3179-H3189.
[10] Taie S, Yokono S, Ueki M, Ogli K. Effects of ulinastatin (urinary trypsin inhibitor) on ATP, intracellular pH, and intracellular sodium transients during ischemia and reperfusion in the rat kidney in vivo. J Anesth 2001; 15: 33-38.
[11] Qin ZS, Tian P, Wu X, Yu HM, Guo N. Effects of ulinastatin administered at different time points on the pathological morphologies of the lung tissues of rats with hyperthermia. Exp Ther Med 2014; 7: 1625-1630.
[12] Tian H, Zhang M, Du C, Li D, Zhou Q, Wu L, Meng F, Song S, Wang L, Lu P, Zhao Z, Yang X. Effects of Rhubarb combined with ulinastatin on T-cell subsets in sepsis rats. Int J Clin Exp Med 2015; 8: 1234-1240.
[13] Lin CS, Liu P, Zhao YJ, Gu MN, Xie FY. [Ulinastatin attenuates lung injury in rats with hemorrhagic shock]. Nan Fang Yi Ke Da Xue Xue Bao 2009; 29: 876-879.
[14] Fang Y, Xu P, Gu C, Wang Y, Fu XJ, Yu WR, Yao M. Ulinastatin improves pulmonary function in severe burn-induced acute lung injury by attenuating inflammatory response. J Trauma 2011; 71: 1297-1304.
[15] Wang L, Luo H, Chen X, Jiang Y, Huang Q. Functional characterization of S100A8 and S100A9 in altering monolayer permeability of human umbilical endothelial cells. PLoS One 2014; 9: e90472.
[16] Whaley JG, Tharakan B, Smith B, Hunter FA, Childs EW. (-)-Deprenyl Inhibits Thermal Injury-Induced apoptotic signaling and hyperpermeability in microvascular endothelial cells. J Burn Care Res 2009; 30: 1018-27.
[17] Childs EW, Tharakan B, Byrge N, Tinsley JH, Hunter FA, Smythe WR. Angiopoietin-1 inhibits intrinsic apoptotic signaling and vascular hyperpermeability following hemorrhagic shock. Am J Physiol Heart Circ Physiol 2008; 294: H2285-H2295.
[18] Wang X, Song R, Chen Y, Zhao M, Zhao KS. Polydatin-a new mitochondria protector for acute severe hemorrhagic shock treatment. Expert Opin Investig Drugs 2013; 22: 169-179.
[19] Zhang XJ, Mei WL, Tan GH, Wang CC, Zhou SL, Huang FR, Chen B, Dai HF, Huang FY. Strophalloside Induces apoptosis of SGC-7901 cells through the mitochondrion-dependent caspase-3 pathway. Molecules 2015; 20: 5714-5728.
[20] Chen TL, Zhu GL, Wang JA, Wang Y, He XL, Jiang J. Apoptosis of bone marrow mesenchymal stem cells caused by hypoxia/reoxygenation via multiple pathways. Int J Clin Exp Med 2014; 7: 4686-4697.
[21] Mao CY, Lu HB, Kong N, Li JY, Liu M, Yang CY, Yang P. Levocarnitine protects H9c2 rat cardiomyocytes from H2O2-induced mitochondrial dysfunction and apoptosis. Int J Med Sci 2014; 11: 1107-1115.
[22] Li T, Liu Y, Li G, Wang X, Zeng Z, Cai S, Li F, Chen Z. Polydatin attenuates ipopolysaccharide-induced acute lung injury in rats. Int J Clin Exp Pathol 2014; 7: 8401-8410.
[23] Li T, Cai S, Zeng Z, Zhang J, Gao Y, Wang X, Chen Z. Protective effect of polydatin against burn-induced lung injury in rats. Respir Care 2014; 59: 1412-1421.
[24] Li JZ, Yu SY, Mo D, Tang XN, Shao QR. Picroside inhibits hypoxia/reoxygenation-induced cardiomyocyte apoptosis by ameliorating mitochondrial function through a mechanism involving a decrease in reactive oxygen species production. Int J Mol Med 2015; 35: 446-452.
[25] Matés JM, Segura JA, Alonso FJ, Márquez J. Oxidative stress in apoptosis and cancer: an update. Arch Toxicol 2012; 86: 1649-1665.
[26] Sinha K, Das J, Pal PB, Sil PC. Oxidative stress: the mitochondria-dependent and mitochondria-independent pathways of apoptosis. Arch Toxicol 2013; 87: 1157-1180.